Neurochemistry International 124 (2019) 31–40

Contents lists available at ScienceDirect

Neurochemistry International

journal homepage: www.elsevier.com/locate/neuint

NADPH oxidase inhibitor apocynin decreases mitochondrial dysfunction and apoptosis in the ventral cochlear nucleus of D-galactose-induced aging model in rats

Zheng-De Du[a,1], Shukui Yu[a,1], Yue Qi[a], Teng-Fei Qu[a], Lu He[a], Wei Wei[b], Ke Liu[a,*], Shu-Sheng Gong[a,**]

[a] Department of Otorhinolaryngology, Beijing Friendship Hospital, Capital Medical University, 95 Yongan Road, Xicheng District, Beijing, 100050, China
[b] Department of Otology, Shengjing Hospital, China Medical University, 36 Sanhao Street, Heping District, Shenyang, 110004, China

ARTICLE INFO

Keywords:
Central presbycusis
NADPH oxidase
Apocynin
Mitochondrial dysfunction
Apoptosis
D-galactose

ABSTRACT

Presbycusis has become a common sensory deficit in humans. Oxidative damage to mitochondrial DNA and mitochondrial dysfunction is strongly associated with the aging of the auditory system. A previous study established a mimetic rat model of aging using D-galactose (D-gal) and first reported that NADPH oxidase-dependent mitochondrial oxidative damage and apoptosis in the ventral cochlear nucleus (VCN) might contribute to D-gal-induced central presbycusis. In this study, we investigated the effects of apocynin, an NADPH oxidase inhibitor, on mitochondrial dysfunction and mitochondria-dependent apoptosis in the VCN of D-gal-induced aging model in rats. Our data showed that apocynin decreased NADPH oxidase activity, H_2O_2 levels, mitochondrial DNA common deletion, and 8-hydroxy-2-deoxyguanosine (8-OHdG) expression and increased total superoxide dismutase (T-SOD) and glutathione peroxidase (GSH-Px) activity in the VCN of D-gal-induced aging model in rats. Moreover, apocynin also decreased the protein levels of phospho-p47^{phox} (p-p47^{phox}), tumor necrosis factor alpha (TNFα), and uncoupling protein 2 (UCP2) in the VCN of D-gal-induced aging model in rats. Meanwhile, apocynin alleviated mitochondrial ultrastructure damage and enhanced ATP production and mitochondrial membrane potential (MMP) levels in the VCN of D-gal-induced aging model in rats. Furthermore, apocynin inhibited cytochrome c (Cyt c) translocation from mitochondria to the cytoplasm and suppressed caspase 3-dependent apoptosis in the VCN of D-gal-induced aging model in rats. Consequently, our findings suggest that neuronal survival promoted by an NADPH oxidase inhibitor is a potentially effective method to enhance the resistance of neurons to central presbycusis.

1. Introduction

Presbycusis, also known as age-related hearing loss, is characterized by the decline of auditory function associated with the age-related degeneration of the peripheral and central auditory systems (Roth, 2015). Central presbycusis refers to age-related degeneration in the auditory portion of the central nervous system, which negatively affects auditory perception or speech discrimination or both (Humes et al., 2012). The cochlear nucleus is the first relay station in the central auditory pathway and consists of two major divisions, the dorsal cochlear nucleus (DCN) and the ventral cochlear nucleus (VCN). They receive the output of the auditory portion of the cochlea and set up parallel analysis and perception (Frisina and Walton, 2006). In our previous study, we found that the activation of NADPH oxidase might be an important source of reactive oxygen species (ROS) in the VCN of D-galactose (D-gal)-induced aging rats. However, the exact effects of NADPH oxidase on the VCN are largely unknown.

Because the tissue of the auditory system is not acquirable from humans during life and because the development of aging, the aging of auditory system, in normal humans and animals is a very slow pross,

Abbreviations: 8-OHdG, 8-hydroxy-2-deoxyguanosine; APO, apocynin; Cyt c, cytochrome c; D-gal, D-galactose; GSH-Px, glutathione peroxidase; p-p47^{phox}, phospho-p47^{phox}; MMP, mitochondrial membrane potential; ROS, reactive oxygen species; TNFα, tumor necrosis factor alpha; T-SOD, total superoxide dismutase; TUNEL, terminal deoxynucleotidyl transferase-mediated deoxyuridine triphosphate nick-end-labeling; VCN, ventral cochlear nucleus; UCP2, uncoupling protein 2

* Corresponding author.
** Corresponding author.
E-mail addresses: liuke@ccmu.edu.cn (K. Liu), gongss1962@163.com (S.-S. Gong).
[1] These authors contributed equally to this work.

https://doi.org/10.1016/j.neuint.2018.12.008
Received 25 October 2018; Received in revised form 1 December 2018; Accepted 17 December 2018
Available online 20 December 2018
0197-0186/

the investigation of presbycusis are relatively limited. Natural aging can be experimentally modelled by the chronic administration of D-gal. Animals treated in this way exhibit poor learning and memory, an attenuated immune response, increased oxidative damage, and dysfunctional mitochondria (Kumar et al., 2009; Lu et al., 2010; Rehman et al., 2017). Mitochondrial DNA is highly susceptible to ROS-induced oxidative damage during the process of aging because of its paucity of protective histones (Druzhyna et al., 2008). Mitochondrial DNA mutations are key players in aging and age-related diseases (Hiona and Leeuwenburgh, 2008). The mitochondrial DNA 4977-bp deletion, also known as the common deletion, in humans and the corresponding mitochondrial DNA 4834-bp deletion in rats are the most frequent aging-associated mitochondrial DNA mutations (Meissner et al., 2008; Yowe and Ames, 1998). Therefore, common deletion has been used as a biomarker for aging. In our previous study, we demonstrated that the expression of NADPH oxidase and the accumulation of common deletion largely increased in the VCN of D-gal-induced aging model in rats (Du Z et al., 2015), but the relationship between NADPH oxidase and common deletion remains unclear.

Aside from mitochondria, the NADPH oxidase system is another main ROS-generating site and is composed of two membrane-bound subunits ($gp91^{phox}$ and $p22^{phox}$) and three cytosolic subunits ($p47^{phox}$, $p67^{phox}$, and $p40^{phox}$). This enzyme transports electrons across the plasma membrane to generate superoxide and downstream ROS (Bedard and Krause, 2007; Leto et al., 2009). Apocynin, also known as acetovanillone, is a selective blocker of NADPH oxidase activity (Kleniewska et al., 2012; Stefanska and Pawliczak, 2008). Currently, its protective role as an oxygen scavenger to reduce oxidative stress and role inhibiting association of $p47^{phox}$ with the membrane heterodimer in leukocytes, monocytes, and endothelial cells have gained much attention (Johnson et al., 2002; Mohammed and Kowluru, 2013; Olukman et al., 2010). In this study, we used D-gal-induced aging model in rats to evaluate the neuroprotective effect of apocynin in the central auditory system. Our hypothesis was that an intraperitoneal administration of apocynin in rats could down-regulate D-gal-induced increased NADPH oxidase activity, prevent NADPH oxidase-dependent mitochondrial oxidative damage and apoptosis in the VCN of D-gal-induced aging model in rats. This study may shed light on the disease etiology of and provide a novel therapeutic target for central presbycusis.

2. Material and methods

2.1. Animals and drug administration

One hundred and four 1-month-old male Sprague-Dawley rats were obtained from the Experimental Animal Centre of Capital Medical University. The rats were housed in a temperature-controlled (20–22 °C) room and had free access to food and drinking water. After acclimation for a week, all rats were randomly allocated into four groups (n = 26 per group): Control group: rats were injected subcutaneously with 0.9% saline (the vehicle of D-gal) once a day for 8 weeks; D-gal group: rats were injected subcutaneously with 500 mg/kg D-gal (Sigma-Aldrich, USA) once a day for 8 weeks (Du Z et al., 2015; Sun et al., 2015); D-gal + vehicle (DMSO) group: rats were injected subcutaneously with 500 mg/kg D-gal and intraperitoneally administered DMSO (Sigma-Aldrich, USA) once a day for 8 weeks (DMSO was used as the vehicle for apocynin at a final concentration of 1% (Lu et al., 2014)); and D-gal + APO group: rats were injected subcutaneously with 500 mg/kg D-gal and intraperitoneally administered 50 mg/kg apocynin (APO; Sigma-Aldrich, USA) (Lu et al., 2014; Song et al., 2013) once a day for 8 weeks. After treatment and behavioral analysis, the rats were killed, and the VCNs were dissected for the determination of NADPH oxidase activity, H_2O_2, total superoxide dismutase (T-SOD) activity, glutathione peroxidase (GSH-Px) activity, ATP, and mitochondrial membrane potential (MMP) levels and the extraction of genomic DNA, protein, and mitochondria. Alternatively, the rats were perfused with 2.5% glutaraldehyde for ultrastructural studies using transmission electron microscopy or with 4% paraformaldehyde for immunohistochemistry and terminal deoxynucleotidyl transferase-mediated deoxyuridine triphosphate nick-end-labeling (TUNEL) staining. All protocols were conformed to the Guide for the Care and Use of Laboratory Animals of the National Institutes of Health. The protocols were approved by the Committee on the Ethics of Animal Experiments of Capital Medical University.

2.2. Behavioral analysis

After D-gal treatment, the spatial learning and memory of 16 rats (n = 8 per group from the Control group and D-gal group) were analyzed by Morris water maze tests. The water maze made up a circular water tank with a 200 cm diameter and 50 cm height. A transparent platform was put inside the tank. The tank was filled with water (23 ± 1 °C) that was made opaque using carbon black ink. At the beginning of each water maze test, a rat was randomly placed in the water at one of the five starting positions facing the wall of the tank. The swim test was terminated when the rat reached the hidden platform or when 120 s had passed. The dwell time was set to 2 s throughout training. If the rat found the platform within 120 s, it was allowed to stay there for 15 s and then sent back to its home cage. If the rat did not find the platform within 120 s, it was guided to the platform and allowed to stay on the platform for 30 s. The rats underwent the test for 5 consecutive days, twice a day, with each session dividing into two trials (intertrial interval = 20 min; intersession interval = 3 h). The mean latency of four trials a day was considered as its mean escape latency. A probe trial (without the platform in the pool) was conducted after the last training session. The rats were allowed to swim for 120 s, and spatial bias was evaluated by dwell time and the swim path length in the pool's quadrants. The percentages of time spent and distance traveled in the target quadrant were applied to statistical analysis (Chen et al., 2008).

2.3. Determination of NADPH oxidase activity

Bilateral VCN tissues were dissected from 24 rats' brains (n = 6 per group) and homogenized in 50 mM phosphate buffer including 1 mM EDTA and 1 mM PMSF. The homogenate was centrifugated at 600 × *g* for 10 min at 4 °C, then the supernatant was collected and centrifuged at 7000 × *g* for 10 min at 4 °C. After centrifugation, the supernatant was collected and used to measure the NADPH oxidase activity. The chemiluminescence assay was used to measure the NADPH oxidase activity (Kashiwagi et al., 1999). Additionally, the lucigenin concentration was 5 μM in the final reaction mixture, and the NADPH oxidase activity was measured based on the amount of superoxide anion produced in the reaction mixture.

2.4. H_2O_2, T-SOD, GSH-Px, and ATP assay

Bilateral VCN tissues from 24 rats' brains (n = 6 per group) were rapidly separated and homogenized in cold saline in closely comparably ways so that paired sample-to-sample comparisons could be made. The right side was used for H_2O_2, T-SOD, and ATP assays, and the left side was used to measure the mitochondrial membrane potential (MMP). The right tissue homogenate was centrifuged at 4000 × *g* for 15 min at 4 °C, and the supernatant was used for H_2O_2, T-SOD, GSH-Px, and ATP assays. Protein concentrations were determined by an Enhanced BCA Protein Assay Kit (Beyotime, China). The levels of H_2O_2, T-SOD, GSH-Px, and ATP in the VCN were quantified by colorimetric kits (Nanjing Jiancheng Bioengineering Institute, China).

2.5. Measurement of MMP

Mitochondria of the VCN were extracted immediately with a Tissue

Mitochondria Isolation Kit (Beyotime, China) and then used for the measurement of MMP. MMP in the VCN was determined by the fluorescent, lipophilic, and cationic JC-1 probe (Nanjing Jiancheng Bioengineering Institute, China) according to the manufacturer's instructions.

2.6. Genomic DNA isolation and determination of common deletion

Both sides of the VCN tissue were departed from 24 rats (n = 6 per group). The right side VCN tissue was used for genomic DNA extraction, and the other side tissue was used for western blotting. A Genomic DNA Isolation Kit was used for total DNA extraction (Tiangen Biotech Co., LTD, China) by the manufacturer's instructions. The DNA concentration of each specimen was determined by using the GeneQuant pro DNA/RNA Calculator (Amersham Pharmacia Biotech, Sweden). TaqMan real-time PCR assay was used for confirm the quantity of common deletion. Due to rare deleted, the D-Loop region can be used to represent the conserved segment. The primers and probes for the D-loop and common deletion were the same as before (Nicklas et al., 2004). Moreover, The PCR amplification was performed on a StepOne™ Real-Time PCR System (Applied Biosystems, USA) in a 20 μl reaction volume. The reaction mixture contained 10 μl of 2 × TaqMan PCR mix (TaKaRa, China), 0.4 μl of 50 × ROX reference dye, 0.4 μl each of forward and reverse primers (10 μM), 0.2 μl of each probe (10 μM), and 4.6 μl of distilled water, 4 μl of the sample DNA (10 ng/μl). And the cycling conditions including an initial phase at 95 °C for 30 s and then 40 cycles at 95 °C for 5 s and 60 °C for 30 s. The cycle number at which a significant increase in the normalized fluorescence was first detected was named as the threshold cycle number (Ct). And the ΔCt (= $Ct_{\text{common deletion}}$ - $Ct_{\text{D-loop}}$) could be used to express the ratio of common deletion. The relative expression (RE) could indicates the factorial difference in the deletions between the experimental and the control group. The RE was calculated as $2^{-\Delta\Delta Ct}$, where ΔΔCt = $\Delta Ct_{\text{common deletion}}$ in the experimental group - $\Delta Ct_{\text{common deletion}}$ in the control group.

2.7. Immunohistochemical analysis

A biomarker of DNA oxidative damage, the levels of 8-hydroxy-2-deoxyguanosine (8-OHdG) (Prabhulkar and Li, 2010), were analyzed by immunohistochemical method. Brains from 16 rats (n = 4 per group) were fixed by 4% buffered paraformaldehyde at 4 °C overnight, dehydrated, and embedded in paraffin wax finally. Subsequently, the brainstem was cut into 5-μm-thick slices at VCN level serially. The VCN tissue from one side was used for immunohistochemical analysis, and the other side of the VCN was used for TUNEL assay. After deparaffining in xylene and rehydrated through graded concentrations of ethanol. After dehydration, samples were incubated with anti-8-OHdG antibody (diluted 1:200; Abcam, USA) and anti-COX IV antibody (diluted 1:100, Proteintech, China) overnight at 4 °C. The slides treated with 8-OHdG antibody so that it could be used to visualize DNA oxidative damage and COX IV antibody to observe mitochondria. After washing in PBS 3 times, they were incubated with Goat Anti-Mouse IgG H&L (Alexa Fluor®488) and Goat Anti-Rabbit IgG H&L (Alexa Fluor®568) as the secondary antibody (diluted 1:500; Abcam, USA) for 1 h at room temperature. Nuclei were counterstained with DAPI staining solution (Beyotime, China). Subsequently, the sections were observed under a laser scanning confocal microscope (Leica TCS SP8, Germany). The expression of 8-OHdG was measured by Image-Pro Plus 6.0 software (Media Cybernetics, Inc., USA). In view of a negative control, sections were treated in the same way, except the omitting of incubation with primary antibody.

2.8. Western blot analysis

The protein expression levels of phospho-$p47^{phox}$ (p-$p47^{phox}$), tumor necrosis factor alpha (TNFα), uncoupling protein 2 (UCP2), cytochrome c (Cyt c), and cleaved caspase-3 (C-cas3) in the VCN were determined via western blot analysis. Cytosolic and mitochondrial fractions were treated with a commercially available cytosol/mitochondria fractionation kit (Beyotime, China) in accordance to the manufacturer's protocol. Protein was extracted using RIPA Lysis and Extraction Buffer (Beyotime, China) following the manufacturer's instructions. An Enhanced BCA Protein Assay Kit (Beyotime, China) was used to determine protein concentrations. Thirty micrograms of each protein lysate were separated by 10% SDS-polyacrylamide gels and then transferred to polyvinylidene difluoride (PVDF) membranes which were incubated for 1 h in a Tris-buffered saline (TBS) with 5% skimmed milk, then washed briefly in TBS, and incubated overnight at 4 °C with the appropriate dilution of antibodies: anti-p-$p47^{phox}$ (diluted 1:500; Invitrogen, USA), anti-$p47^{phox}$ (diluted 1:500; Abcam, USA), anti-TNFα (diluted 1:1000, Cell Signaling Technology, USA), anti-UCP2 (diluted 1:500; Abcam, USA), anti-Cyt c (diluted 1:500; Abcam, USA), or anti-C-cas3 (diluted 1:1000; Cell Signaling Technology, USA). After washing the membranes, the membranes were incubated for 1 h at room temperature with the appropriate horseradish peroxidase (HRP)-conjugated secondary antibody (diluted 1:5000; ZSGB-BIO, China). Furthermore, membranes were visualized using BeyoECL Plus (Beyotime, China). Quantitation of the detected bands was performed with Image-Pro Plus 6.0 software as previously described (Media Cybernetics, Inc., USA). β-actin was used as an internal control for total protein, and COX IV was used as an internal control for mitochondrial protein.

2.9. Transmission electron microscopy

Transmission electron microscopy was used to performe the ultrastructure of mitochondria in the VCN. Sixteen rats (n = 4 per group) were sacrificed, and both sides of the VCN from each rat were perfused with 2.5% glutaraldehyde overnight at 4 °C. After incubating in 1% osmium tetroxide for 2 h at room temperature for post-fixation, the tissues were dehydrated in the graded ethanol and acetone series, immersed in an acetone/Epon 812 mixture for 2 h and then in Epon 812 for 2 h, and embedded in Epon 812 for 10 h at 80 °C finally. Serial ultrathin sections (50 nm) were placed onto copper grids and stained with uranyl acetate followed by lead citrate. The ultrastructure was measured under a transmission electron microscope (JEM-2100, JEOL Ltd., Tokyo, Japan).

2.10. TUNEL staining

Apoptotic cells were detected in situ by TUNEL staining (TUNEL POD kit; Roche Molecular Biochemicals, Germany). Briefly, a section was deparaffinized and rehydrated. After treatment with proteinase K (20 μg/ml in 10 mM Tris-HCl, pH 7.6) for 15 min at 37 °C, the sections were washed with PBS, and the labelling reaction was performed by a labelling solution containing terminal deoxynucleotidyl transferase, its buffer and fluorescein deoxyuridine triphosphate at 37 °C for 1 h in a humidity chamber. After washing with PBS, each section was examined under a fluorescence microscope (Leica DM2500, Germany). For the number of TUNEL-positive stained cells, it was counted using Image-Pro Plus 6.0 software (Media Cybernetics, Inc., USA).

2.11. Statistical analysis

All the data are presented as the mean ± standard deviation (SD). Statistical tests were performed with SPSS 13.0 software (SPSS Inc., USA). The data on memory impairment were analyzed via independent-samples t-tests, whereas the other data were analyzed using one-way ANOVA. Therefore, the least significant difference (LSD) post hoc test was used to evaluate the differences between groups. Of all these, differences with a $P < 0.05$ were considered to be statistically significant.

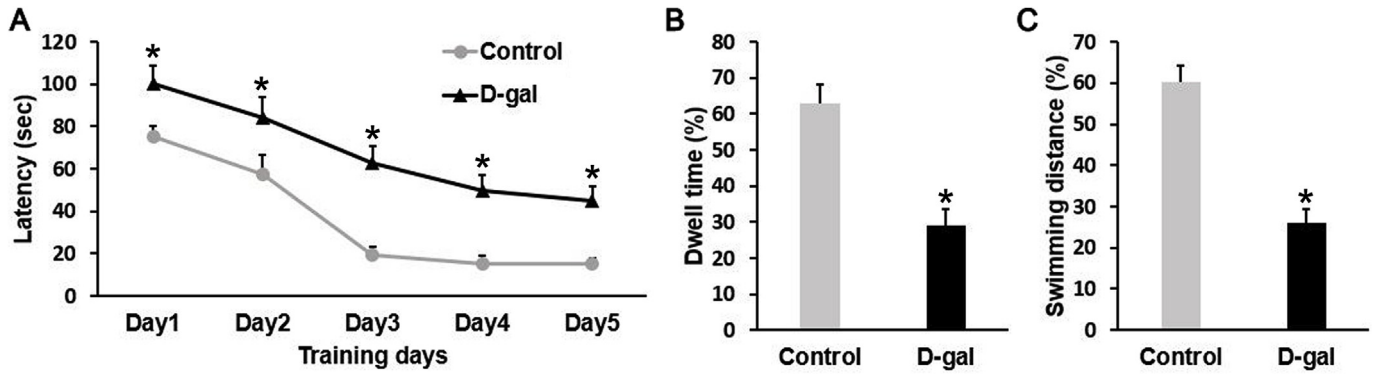

Fig. 1. Spatial learning and memory of rats in the D-gal group and the Control group. (A) Histogram of the mean escape latency time during training. (B) The percentage of time spent in the target quadrant during probe tests immediately after the end of acquisition training. (C) The percentage of distance traveled in the target quadrant during probe tests immediately after the end of acquisition training. Data are expressed as the mean ± SD. *$P < 0.01$ versus the Control group.

3. Results

3.1. Memory impairment in D-gal-induced aging model in rats

To confirm the establishment of the aging model induced by D-gal treatment, the spatial learning and memory of rats in the D-gal group and Control group were observed using Morris water maze tests. As shown in Fig. 1A, the mean latency to find the platform decreased gradually during training days in the D-gal group and the Control group. However, the D-gal group showed longer latencies to the platform than the Control group ($P < 0.01$). Next, Fig. 1B illustrates the significant difference in the percentage of time spent in the target quadrant between the D-gal group and the Control group ($P < 0.01$). Finally, Fig. 1C illustrates the significant difference found in the percentage of distance traveled in the target quadrant between the D-gal and the Control group ($P < 0.01$). These results show the impaired spatial learning and memory ability in D-gal-induced aging model in rats.

3.2. Apocynin alleviates NADPH oxidase-associated oxidative stress in the VCN of D-gal-induced aging model in rats

To investigate the effects of the NADPH oxidase inhibitor apocynin on oxidative stress in the VCN of D-gal-induced aging model in rats, we measured the levels of NADPH oxidase activity, H_2O_2, T-SOD and GSH-Px activity. As shown in Fig. 2A, the levels of NADPH oxidase activity in the Control group, D-gal group, D-gal + DMSO group, and D-gal + APO group were 300.67 ± 61.22 μmol/mg/min, 1208.67 ± 182.34 μmol/mg/min, 1135.67 ± 171.73 μmol/mg/min, and 589.17 ± 126.51 μmol/mg/min, respectively. The level of NADPH oxidase activity in the D-gal group was significantly higher than that in the Control group ($P < 0.01$). The level of NADPH oxidase activity in the D-gal + APO group was significantly lower than that in the D-gal group ($P < 0.01$). There was no significant difference between the D-gal group and the D-gal + DMSO group. As shown in Fig. 2B, the levels of H_2O_2 in the Control group, D-gal group, D-gal + DMSO group, and D-gal + APO group were 15.01 ± 1.65 mmol/g protein, 32.71 ± 2.15 mmol/g protein, 32.45 ± 2.04 mmol/g protein, and 19.71 ± 2.80 mmol/g protein, respectively. The level of H_2O_2 in the D-gal group was significantly higher than that in the Control group ($P < 0.01$). The level of H_2O_2 in the D-gal + APO group was significantly lower than that in the D-gal group ($P < 0.01$). There was no significant difference between the D-gal group and the D-gal + DMSO group. As shown in Fig. 2C, the levels of T-SOD activity in the Control group, D-gal group, D-gal + DMSO group, and D-gal + APO group were 134.36 ± 14.72 U/mg protein, 73.61 ± 5.89 U/mg protein, 74.70 ± 8.62 U/mg protein, and 105.49 ± 10.95 U/mg protein, respectively. The level of T-SOD activity in the D-gal group was significantly lower than that in the Control group ($P < 0.01$). The level of T-SOD activity in the D-gal + APO group was significantly higher than that in the D-gal group ($P < 0.01$). There was no significant difference between the D-gal group and the D-gal + DMSO group. As shown in Fig. 2D, the levels of GSH-Px activity in the Control group, D-gal group, D-gal + DMSO group, and D-gal + APO group were 18.24 ± 1.05 U/mg protein, 7.53 ± 0.77 U/mg protein, 7.4 ± 0.87 U/mg protein, and 12.51 ± 1.57 U/mg protein, respectively. The level of GSH-Px activity in the D-gal group was significantly lower than that in the Control group ($P < 0.01$). The level of GSH-Px activity in the D-gal + APO group was significantly higher than that in the D-gal group ($P < 0.01$). There was no significant difference between the D-gal group and the D-gal + DMSO group. Thus, these findings indicated that apocynin decreased NADPH oxidase-associated oxidative stress in the VCN of D-gal-induced aging model in rats.

3.3. Apocynin alleviates mitochondrial DNA damage in the VCN of D-gal-induced aging model in rats

To investigate the effect of the NADPH oxidase inhibitor apocynin on mitochondrial DNA oxidative damage in the VCN of D-gal-induced aging model in rats, we measured the expression of 8-OHdG (a biomarker of DNA oxidative damage) and the accumulation of common deletion. As shown in Fig. 3A, the expression of 8-OHdG (red) was mainly in the mitochondria (green) of neurons of the VCN of the D-gal group and D-gal + DMSO group. The levels of 8-OHdG in the D-gal group, D-gal + DMSO group, and D-gal + APO group were 4.90 ± 0.83-fold, 4.81 ± 0.97-fold, and 1.98 ± 0.49-fold compared with that in the Control group, respectively. The level of 8-OHdG in the D-gal group was significantly higher than that in the Control group ($P < 0.01$). The level of 8-OHdG in the D-gal + APO group was significantly lower than that in the D-gal group ($P < 0.01$). There was no significant difference between the D-gal group and the D-gal + DMSO group (Fig. 3B). As shown in Fig. 3C, the levels of common deletion in the D-gal group, D-gal + DMSO group, and D-gal + APO group were 2.45 ± 0.36-fold, 2.30 ± 0.35-fold, and 1.51 ± 0.25-fold compared with that in the Control group. The levels of common deletion in the D-gal group were significantly higher than that in the Control group ($P < 0.01$). The level of common deletion in the D-gal + APO group was significantly lower than that in the D-gal group ($P < 0.01$). There was no significant difference between the D-gal group and the D-gal + DMSO group. These findings indicated that apocynin largely alleviates mitochondrial DNA oxidative damage in the VCN of D-gal-induced aging model in rats.

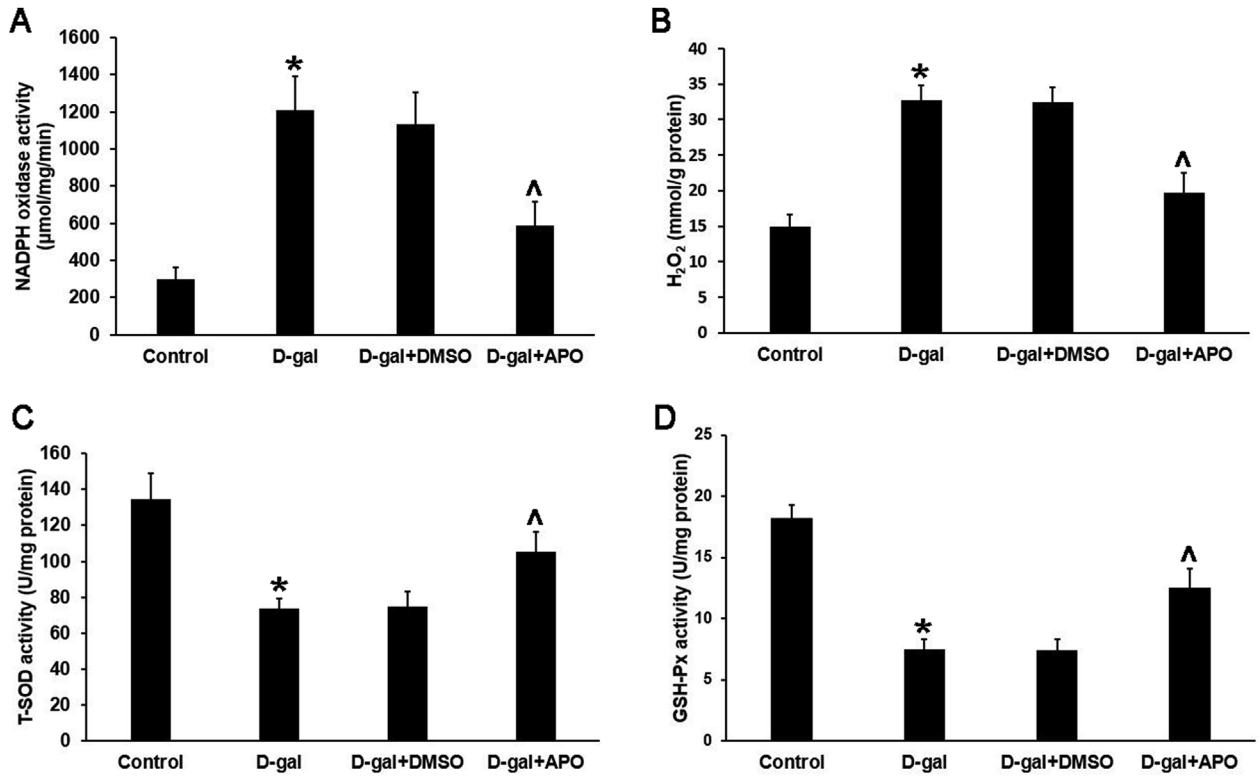

Fig. 2. The levels of NADPH oxidase activity, H_2O_2, T-SOD and GSH-Px **activity in the VCN of rats in the different groups.** (A) Levels of NADPH oxidase activity in the VCN of rats in the different groups. (B) Levels of H_2O_2 in the VCN of rats in the different groups. (C) Levels of T-SOD activity in the VCN of rats in the different groups. (D) Levels of GSH-Px activity in the VCN of rats in the different groups. Data are expressed as the mean ± SD. *$P < 0.01$ versus the Control group; ^$P < 0.01$ versus the D-gal group. T-SOD, total superoxide dismutase; GSH-Px, glutathione peroxidase.

3.4. Apocynin decreases the protein expression of p-p47^{phox}, TNFα, and UCP2 in the VCN of D-gal-induced aging model in rats

To evaluate the protein levels of p-p47^{phox}, TNFα, and UCP2 in the VCN of the different groups, western blot analysis was performed. As shown in Fig. 4, the protein levels of p-p47^{phox} in the D-gal group, D-gal + DMSO group, and D-gal + APO group were 3.88 ± 0.56-fold, 3.74 ± 0,21-fold, and 1.99 ± 0.37-fold compared with that in the Control group, respectively; the protein levels of TNFα in the D-gal group, D-gal + DMSO group, and D-gal + APO group were 6.58 ± 0.75-fold, 6.50 ± 1.13-fold, and 2.44 ± 0.86-fold compared with that in the Control group, respectively; the protein levels of UCP2 in the D-gal group, D-gal + DMSO group, and D-gal + APO group were 4.79 ± 0.54-fold, 5.24 ± 0.67-fold, and 2.77 ± 0.37-fold compared with that in the Control group, respectively. The protein levels of p-p47^{phox}, TNFα, and UCP2 in the D-gal group were significantly higher than those in the Control group ($P < 0.01$). The protein levels of p-p47^{phox}, TNFα, and UCP2 in the D-gal + APO group were significantly lower than those in the D-gal group ($P < 0.01$). There was no significant difference between the D-gal group and the D-gal + DMSO group.

3.5. Apocynin protects the mitochondrial ultrastructure in the VCN of D-gal-induced aging model in rats

To investigate the effect of the NADPH oxidase inhibitor apocynin on the mitochondrial structure in the VCN of D-gal-induced aging model in rats, we assessed the mitochondrial ultrastructure using transmission electron microscopy. As shown in Fig. 5A, E, the shape and size of mitochondria in the VCN of rats from the Control group were normal. In contrast, numerous mitochondria in the VCN of rats from the D-gal group were swollen with a reduced electron density in the matrix or had undergone serious degeneration (Fig. 5B and C). Additionally, lipofuscin granules frequently appeared in the cytoplasm of neurons in the VCN of rats from the D-gal group (Fig. 5D). In the D-gal + APO group (Fig. 5F, G, H), the shape and size of mitochondria in the VCN of rats were close to normal; some mitochondria appeared only a little swollen, and less lipofuscin was observed in the cytoplasm of neurons in the VCN of rats.

3.6. Apocynin improves mitochondrial function in the VCN of D-gal-induced aging model in rats

To further characterize the effect of the NADPH oxidase inhibitor apocynin on mitochondrial function in the VCN of D-gal-induced aging model in rats, we detected the levels of ATP and MMP. As shown in Fig. 6A, the levels of ATP in the Control group, D-gal group, D-gal + DMSO group, and D-gal + APO group were 13.26 ± 1.07 nmol/mg protein, 6.58 ± 0.99 nmol/mg protein, 7.20 ± 2.21 nmol/mg protein, and 10.56 ± 1.34 nmol/mg protein, respectively. The level of ATP in the D-gal group was significantly lower than that in the Control group ($P < 0.01$). The level of ATP in the D-gal + APO group was significantly higher than that in the D-gal group ($P < 0.01$). There was no significant difference between the D-gal group and the D-gal + DMSO group. As shown in Fig. 6B, the levels of MMP in the Control group, D-gal group, D-gal + DMSO group, and D-gal + APO group were 8.25 ± 0.88, 5.05 ± 0.63, 5.42 ± 0.85, and 7.45 ± 0.96, respectively. The level of MMP in the D-gal group was significantly lower than that in the Control group ($P < 0.01$). The level of MMP in the D-gal + APO group was significantly higher than that in the D-gal group ($P < 0.01$). There was no significant difference between the D-gal group and the D-gal + DMSO group.

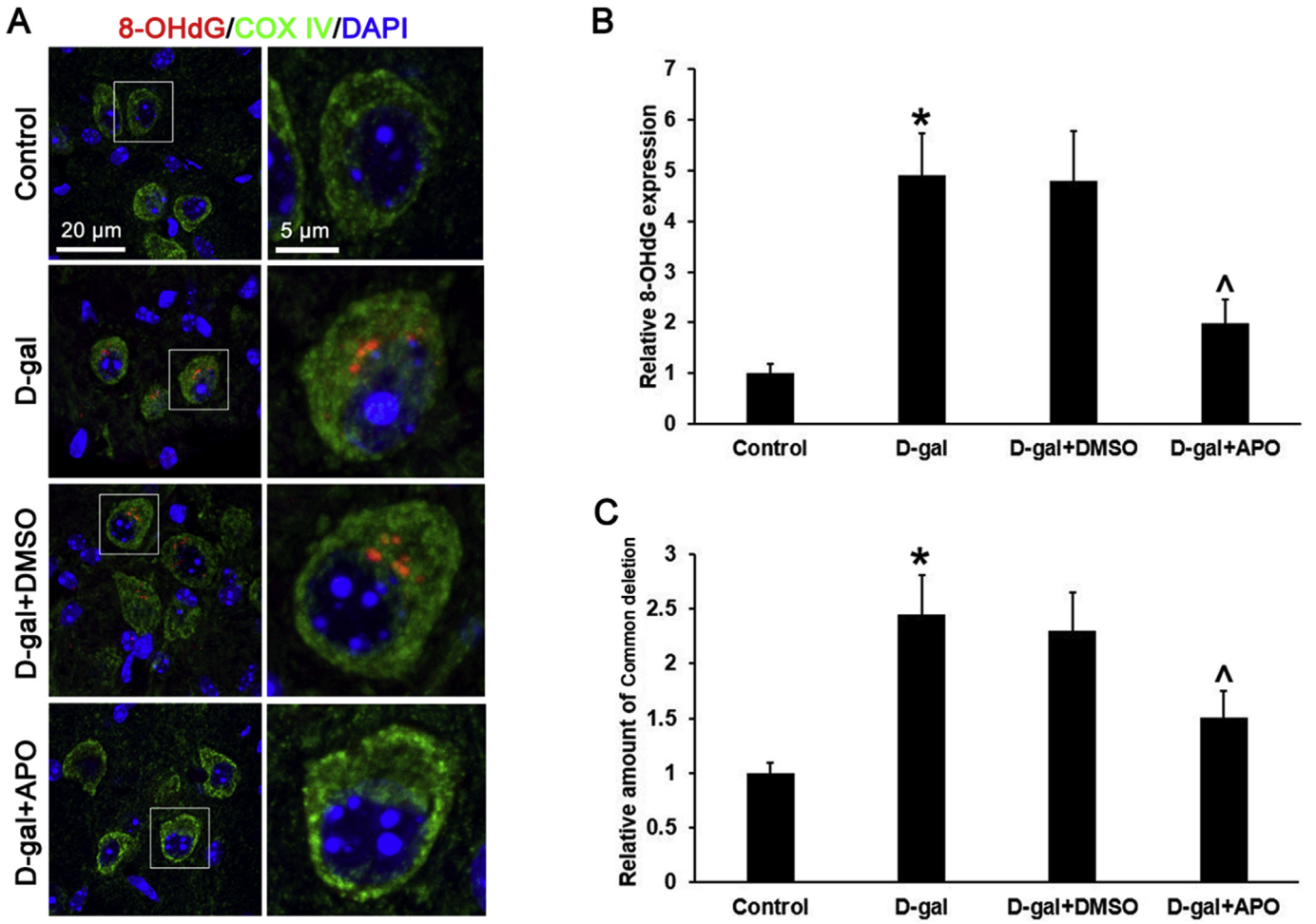

Fig. 3. The levels of 8-OHdG and common deletion in the VCN of rats in the different groups. (A) The expression and localization of 8-OHdG in the VCN of rats in the different groups using immunohistochemical staining. (B) Quantitative assessment of 8-OHdG expression in the VCN of rats in the different groups. (C) Levels of common deletion in the VCN of rats in the different groups. Data are expressed as the mean ± SD. *$P < 0.01$ versus the Control group; ^$P < 0.01$ versus the D-gal group. Scale bar = 20 μm or 5 μm. 8-OHdG, 8-hydroxy-2-deoxyguanosine.

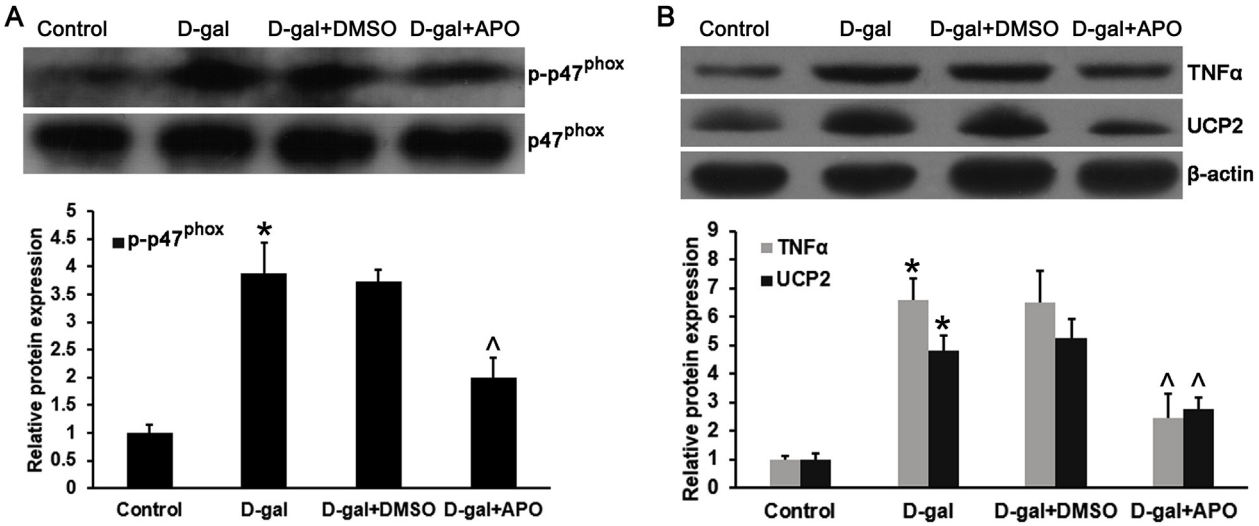

Fig. 4. Protein expression of p-p47^{phox}, TNFα, and UCP2 in the VCN of rats in the different groups. (A) Protein expression of p-p47^{phox} in the VCN of rats in the different groups. (B) Protein expression of TNFα and UCP2 in the VCN of rats in the different groups. Data are expressed as the mean ± SD. *$P < 0.01$ versus the Control group; ^$P < 0.01$ versus the D-gal group. p-p47^{phox}, phosphos-p47^{phox}; TNFα, tumor necrosis factor alpha; UCP2, uncoupling protein 2.

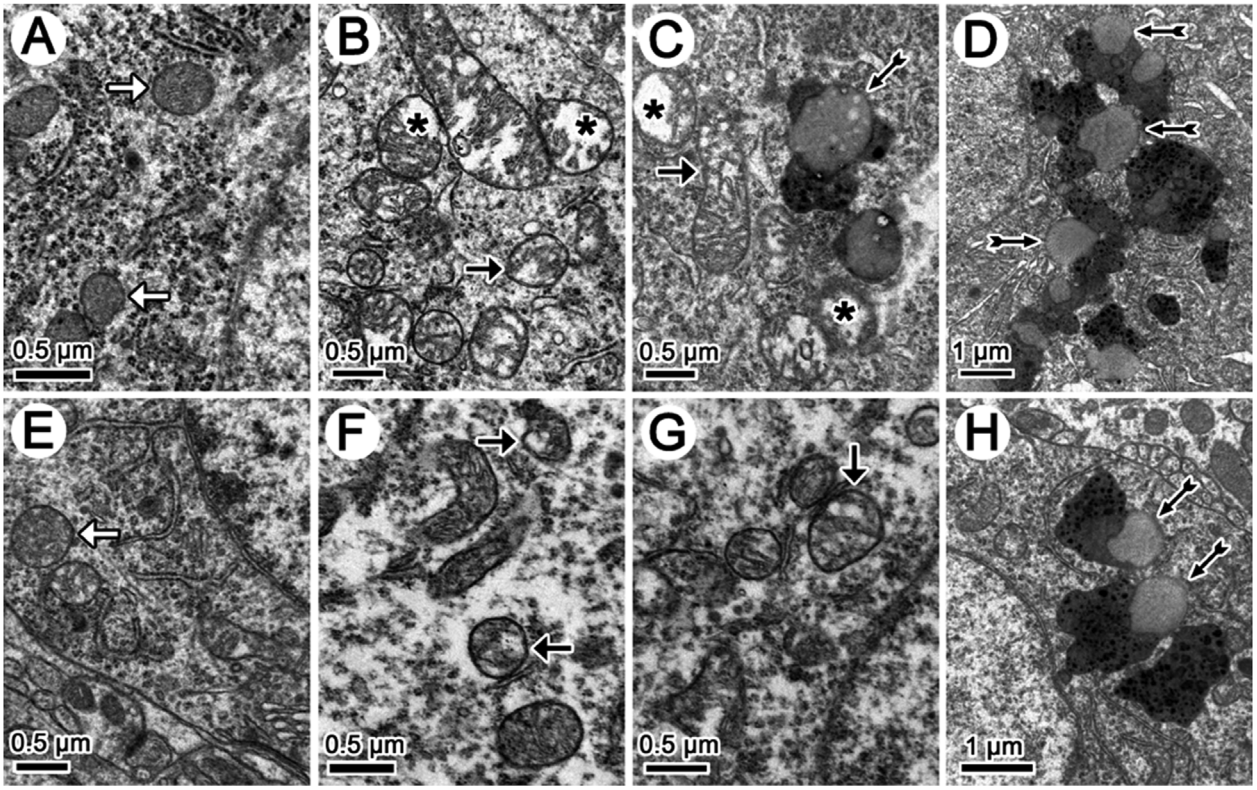

Fig. 5. Mitochondrial ultrastructure in the VCN of rats in the different groups. (A, E) Normal mitochondria (white arrows) in the Control group. (B, C, D) Swollen mitochondria with reduced electron density (black arrows), vacuolar mitochondria (asterisks), and lipofuscin granules (double arrows) in the D-gal group. (F, G, H) Less swollen mitochondria with reduced electron density (black arrows) and lipofuscin granules (double arrows) in the D-gal + APO group compared to those in the D-gal group. A, B, C, E, F, and G: Scale bar = 0.5 μm; D and H: Scale bar = 1 μm.

3.7. Apocynin inhibits mitochondria-dependent apoptosis in the VCN of D-gal-induced aging model in rats

To determine the effects of the NADPH oxidase inhibitor apocynin on mitochondria-dependent apoptosis in the VCN of D-gal-induced aging model in rats, we detected mitochondrial and cytoplasmic Cyt c protein levels using western blot analysis. As shown in Fig. 7A, the mitochondrial protein levels of Cyt c in the D-gal group, D-gal + DMSO group, and D-gal + APO group were 0.27 ± 0.10-fold, 0.29 ± 0.12-fold, and 0.63 ± 0.22-fold compared with that in the Control group, respectively. The mitochondrial protein levels of Cyt c in the D-gal group were significantly lower than that in the Control group ($P < 0.01$). The mitochondrial protein levels of Cyt c in the D-gal + APO group were significantly higher than that in the D-gal group ($P < 0.01$). As shown in Fig. 7B, the cytoplasmic protein levels of Cyt c in the D-gal group, D-gal + DMSO group, and D-gal + APO group were 9.14 ± 1.05-fold, 8.96 ± 1.59-fold, and 3.41 ± 0.88-fold compared with that in the Control group, respectively. The cytoplasmic protein levels of Cyt c in the D-gal group were significantly higher than that in the Control group ($P < 0.01$). The cytoplasmic protein levels of Cyt c in the D-gal + APO group were significantly lower than that in the D-gal group ($P < 0.01$). There was no significant difference between the D-gal group and the D-gal + DMSO group. Thus, these findings indicated that apocynin inhibits Cyt c translocation from mitochondria to the cytoplasm in the VCN of D-gal-induced aging model in rats.

To further investigate the effect of the NADPH oxidase inhibitor apocynin on mitochondria-dependent apoptosis in the VCN of D-gal-induced aging model in rats, we detected C-cas3 protein levels using

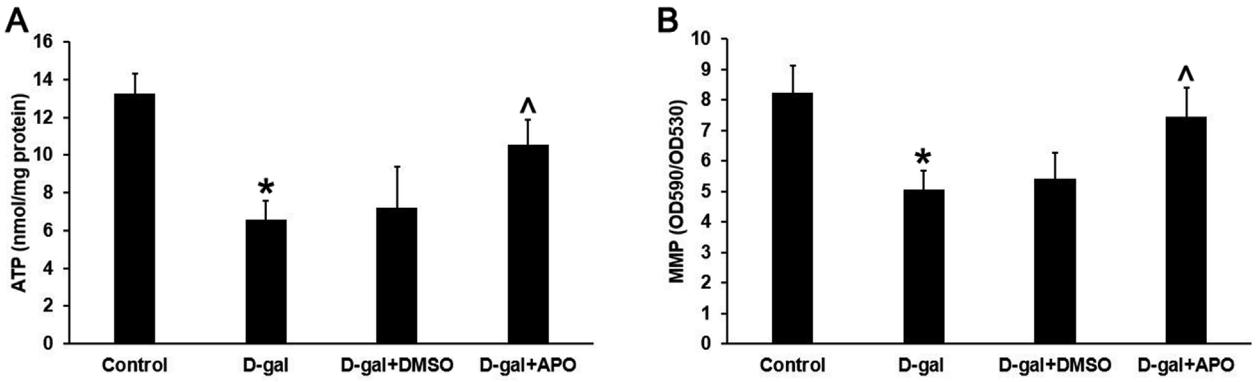

Fig. 6. Mitochondrial function in the VCN of rats in the different groups. (A) Levels of ATP in the VCN of rats in the different groups. (B) Levels of MMP in the VCN of rats in the different groups. Data are expressed as the mean ± SD. *$P < 0.01$ versus the Control group; ^$P < 0.01$ versus the D-gal group. MMP, mitochondrial membrane potential.

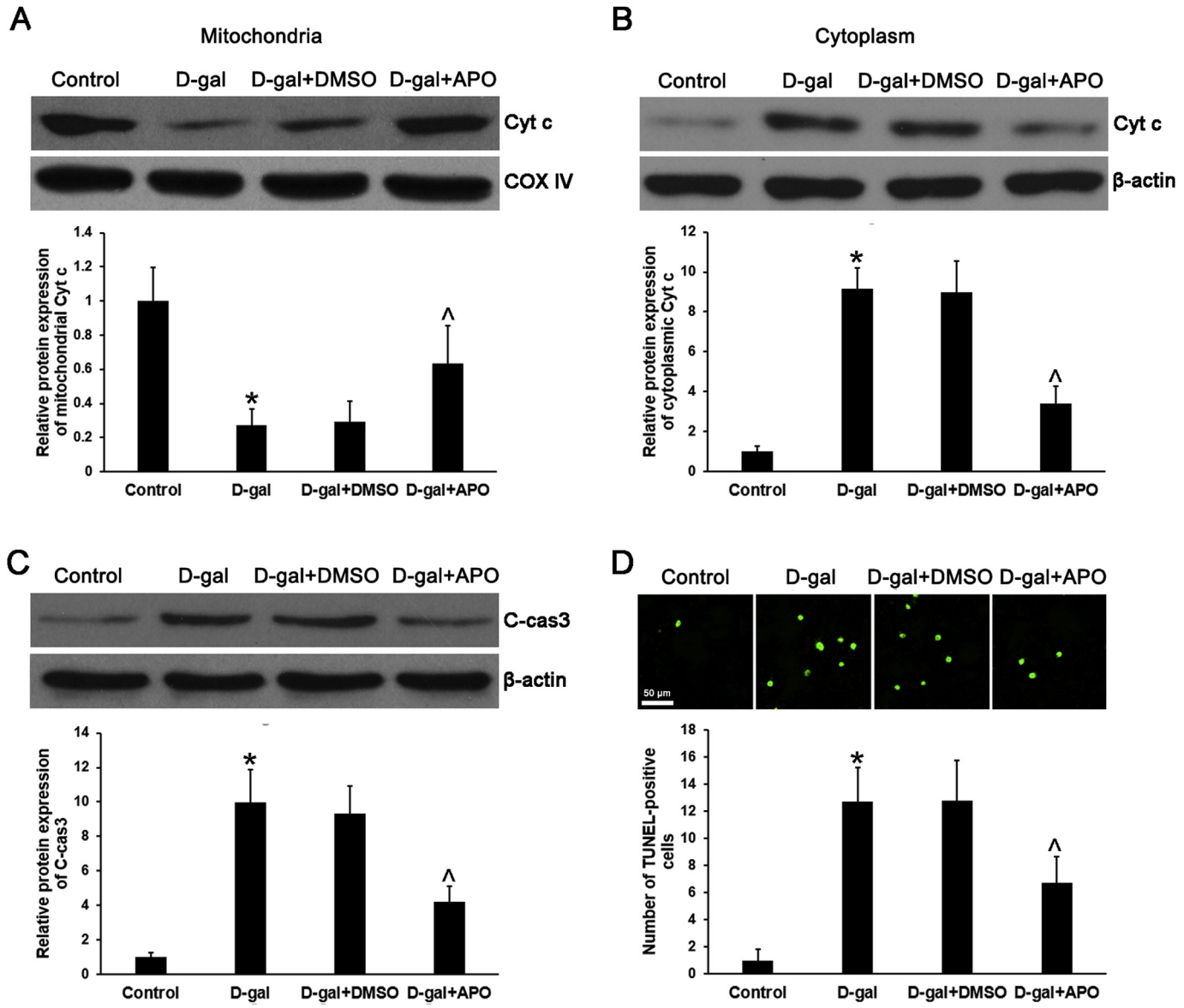

Fig. 7. Mitochondria-dependent apoptosis in the VCN of rats in the different groups. (A) The protein expression of mitochondrial Cyt c in the VCN of rats in the different groups using western blotting. (B) The protein expression of cytoplasmic Cyt c in the VCN of rats in the different groups using western blotting. (C) The protein expression of C-cas3 in the VCN of rats in the different groups using western blotting. (D) Apoptotic cells in the VCN of rats in the different groups using TUNEL staining. Data are expressed as the mean ± SD. *$P < 0.01$ versus the Control group; ^$P < 0.01$ versus the D-gal group. Scale bar = 50 μm. Cyt c, cytochrome c; C-cas3, cleaved caspase 3; TUNEL, terminal deoxynucleotidyl transferase-mediated deoxyuridine triphosphate nick-end-labeling.

western blot analysis (Fig. 7C) and apoptotic cells in situ using TUNEL staining (Fig. 7D). As shown in Fig. 7C, the protein levels of C-cas3 in the D-gal group, D-gal + DMSO group, and D-gal + APO group were 9.99 ± 1.87-fold, 9.34 ± 1.58-fold, and 4.21 ± 0.90-fold compared with that in the Control group, respectively. The protein levels of C-cas3 in the D-gal group were significantly higher than that in the Control group ($P < 0.01$). The protein levels of C-cas3 in the D-gal + APO group were significantly lower than that in the D-gal group ($P < 0.01$). As shown in Fig. 7D, the numbers of TUNEL-positive cells in the Control group, D-gal group, D-gal + DMSO group, and D-gal + APO group were 1.00 ± 0.82, 12.75 ± 2.5, 12.80 ± 2.94, and 6.75 ± 1.89, respectively. The number of TUNEL-positive cells in the D-gal group was significantly higher than that in the Control group ($P < 0.01$). The number of TUNEL-positive cells in the D-gal + APO group was significantly lower than that in the D-gal group ($P < 0.01$). There was no significant difference between the D-gal group and the D-gal + DMSO group. These findings further indicated that apocynin inhibits the activation of the mitochondria-dependent apoptotic pathway in the VCN of D-gal-induced aging model in rats.

4. Discussion

It was reported that D-gal can induce memory loss, oxidative stress, and mitochondrial damage, similar to what occurs in natural aging in rats. Therefore, D-gal has been used as an animal aging model for aging and anti-aging research (Chen et al., 2010; Li et al., 2018; Rehman et al., 2017). In our study, the rats treated with D-gal exhibited significantly impaired performance in water maze tests coupled with oxidative stress, mitochondrial DNA common deletion accumulation, and mitochondrial ultrastructure damage in the VCN. These findings demonstrated that the chronic administration of D-gal induced aging in the VCN of the central auditory system of rats. Currently, the increase in life expectancy has resulted in an increase in the prevalence of presbycusis. We used D-gal-induced aging model in rats to investigate the

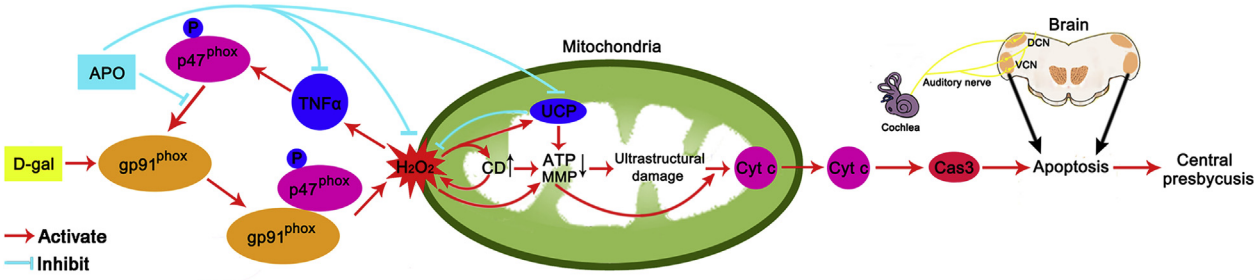

Fig. 8. Schematic diagram of the protective effects of APO against D-gal-induced central presbycusis. APO decreases D-gal-induced p-p47^{phox}, TNFα, and UCP overexpression, and alleviates NADPH oxidase-associated mitochondrial oxidative damage and mitochondrial dysfunction, and inhibits mitochondria-dependent apoptosis in the VCN of rats, and finally prevents central presbycusis. APO, apocynin; Cas3, caspase 3; CD, common deletion; Cyt c, cytochrome c; DCN, dorsal cochlear nucleus; D-gal, D-galactose; MMP, mitochondrial membrane potential; P, phosphorylation; TNFα, Tumor necrosis factor alpha; UCP, uncoupling protein; VCN, ventral cochlear nucleus.

neuroprotective role and possible mechanism of the NADPH oxidase inhibitor apocynin in reducing D-gal-induced NADPH oxidase-associated oxidative stress, mitochondrial damage, and mitochondria-dependent apoptosis in the VCN, parameters related to the aging of the central auditory system.

In addition to mitochondria, NADPH oxidase is a main source of ROS in the aging process of the auditory system and might be responsible for oxidative stress in the inner ear (Du Z et al., 2012a), VCN (Du Z et al., 2015), and hippocampus (Du Z et al., 2012b). In our previous study, we demonstrated that the overexpression of NADPH oxidase 2 (also known as gp91^{phox}) and its corresponding subunits (p22^{phox}, p47^{phox}, and p67^{phox}) might contribute to the increase in mitochondrial oxidative damage and the decrease in ATP production and MMP and lead to the activation of the mitochondria-dependent apoptotic pathway in the VCN of D-gal-induced aging model in rats (Du Z et al., 2015). In this study, we found that the administration of the NADPH oxidase inhibitor apocynin decreased the level of NADPH oxidase activity, H_2O_2 production, and mitochondrial DNA oxidative damage and increased the level of T-SOD and GSH-Px activity in the VCN of D-gal-induced aging model in rats. Our current results suggest that apocynin efficiently decreased NADPH oxidase-associated oxidative stress in the VCN of D-gal-induced aging model in rats.

According to the western blot results, apocynin also prevented D-gal-induced p-p47^{phox}, TNFα, and UCP2 protein overexpression in the VCN of rats. Phosphorylation of p47^{phox} is a key event in NADPH oxidase activation (el et al., 1994; El et al., 1996; Okamura et al., 1988; Rotrosen and Leto, 1990), and previous studies demonstrated that apocynin inhibited p47^{phox} activation (Dang et al., 2016) and that TNFα induced clear p47^{phox} phosphorylation (Dewas et al., 2003). Moreover, mitochondrial uncoupling by UCP2 can be activated by ROS. The mild uncoupling caused by the activation of UCP2 may decrease the proton-motive force and attenuate mitochondrial ROS production at the cost of efficient ATP synthesis (Divakaruni and Brand, 2011; Mailloux and Harper, 2011; Toda and Diano, 2014). Therefore, apocynin alleviates NADPH oxidase-associated oxidative stress in the VCN of D-gal-induced aging model in rats via regulating the expression of p-p47^{phox}, TNFα, and UCP2.

Oxidative stress and the accumulation of mitochondrial DNA mutations have a strong association with the molecular process of aging (Harman, 2001; Hiona and Leeuwenburgh, 2008). Common deletion is the most frequent age-associated mitochondrial DNA mutation, and it has been used as a biomarker for aging (Meissner et al., 2008; Nicklas et al., 2004; Yowe and Ames, 1998). The association between elevated common deletion and presbycusis has been observed in a number of studies (Bai et al., 1997; Chen et al., 2010; Markaryan et al., 2009; Ueda et al., 1998). The accumulation of common deletion in the tissue of the auditory system may lead to mitochondrial dysfunction, resulting in increased mitochondrial ROS generation and decreased ATP production and MMP (Harman, 2001; Hiona and Leeuwenburgh, 2008). In this study, we demonstrated for the first time that apocynin efficiently decreased the accumulation of common deletion and improved mitochondrial function in the VCN of D-gal-induced aging model in rats.

Mitochondrial dysfunction and mitochondrial ultrastructure damage may initiate apoptosis by releasing pro-apoptotic factors, such as Cyt c, from the mitochondrial intermembrane space into the cytoplasm to trigger the mitochondria-dependent apoptosis pathway (Green and Kroemer, 2004; Hengartner, 2000). In this study, we demonstrated that apocynin efficiently blocked the translocation of Cyt c from mitochondria to the cytoplasm. To further investigate the effect of apocynin on mitochondria-dependent apoptosis in the VCN of D-gal-induced aging model in rats, we measured a key effector protease in the mitochondrial pathway of apoptosis, C-cas3 (Green and Kroemer, 2004), and the number of apoptotic cells in situ by TUNEL staining. We found that apocynin significantly decreased the protein level of C-cas3 and the number of apoptotic cells in the VCN of D-gal-induced aging model in rats. A recent study also demonstrated that apocynin attenuated mitochondrial dysfunction and mitochondria-dependent apoptosis via inhibition of harmful ROS following ischemic injury in the rat brain (Kapoor et al., 2018). Consequently, these findings suggest that the NADPH oxidase inhibitor apocynin prevents the activation of the mitochondrial pathway of apoptosis not only through blocking the translocation of Cyt c from mitochondria to the cytoplasm but also through suppressing the protein expression of C-cas3. However, we also found that apocynin did not totally eliminate apoptotic cells, indicating that, in addition to the mitochondrial pathway of apoptosis, there might be other apoptotic pathways involved in the VCN of D-gal-induced aging model in rats.

5. Conclusions

Based on the current results, we concluded the following (Fig. 8): (1) D-gal injection induces oxidative stress, mitochondrial dysfunction, and apoptosis in the VCN and mimics the biologic aging process of the central auditory system. (2) NADPH oxidase-associated ROS generation is responsible for mitochondrial dysfunction and mitochondria-dependent apoptosis in the VCN of D-gal-induced aging model in rats. (3) The NADPH oxidase inhibitor apocynin protects neurons in the VCN of D-gal-induced aging model in rats via decreasing ROS generation, improving mitochondrial function, and blocking the mitochondrial pathway of apoptosis. (4) Although apocynin did not totally eliminate apoptotic cells, it largely improved mitochondrial function and reduced apoptotic cells in the VCN of D-gal-induced aging. Apocynin may be a useful therapeutic agent to prevent or slow the development of central presbycusis.

Acknowledgements

This work was supported by grants from National Natural Science

Foundation of China (Nos. 81700917 and 81771016), China Postdoctoral Science Foundation (No. 2018M630180), Science, Technology and Innovation Commission of Shenzhen Municipality of China (No. JCYJ20160429181957912), Shenzhen Nanshan District Science and Technology Key Program of China (No. 2016004) and Beijing Natural Science Foundation of China (No. 7174291).

References

Bai, U., Seidman, M.D., Hinojosa, R., Quirk, W.S., 1997. Mitochondrial DNA deletions associated with aging and possibly presbycusis: a human archival temporal bone study. Am. J. Otol. 18, 449–453.
Bedard, K., Krause, K.H., 2007. The NOX family of ROS-generating NADPH oxidases: physiology and pathophysiology. Physiol. Rev. 87, 245–313.
Chen, B., Zhong, Y., Peng, W., Sun, Y., Kong, W.J., 2010. Age-related changes in the central auditory system: comparison of D-galactose-induced aging rats and naturally aging rats. Brain Res. 1344, 43–53.
Chen, C., Lang, S., Zuo, P., Yang, N., Wang, X., 2008. Treatment with dehydroepiandrosterone increases peripheral benzodiazepine receptors of mitochondria from cerebral cortex in D-galactose-induced aged rats. Basic Clin. Pharmacol. Toxicol. 103, 493–501.
Dang, D.K., Shin, E.J., Nam, Y., Ryoo, S., Jeong, J.H., Jang, C.G., Nabeshima, T., Hong, J.S., Kim, H.C., 2016. Apocynin prevents mitochondrial burdens, microglial activation, and pro-apoptosis induced by a toxic dose of methamphetamine in the striatum of mice via inhibition of p47phox activation by ERK. J. Neuroinflammation 13, 12.
Dewas, C., Dang, P.M., Gougerot-Pocidalo, M.A., El-Benna, J., 2003. TNF-alpha induces phosphorylation of p47(phox) in human neutrophils: partial phosphorylation of p47phox is a common event of priming of human neutrophils by TNF-alpha and granulocyte-macrophage colony-stimulating factor. J. Immunol. 171, 4392–4398.
Divakaruni, A.S., Brand, M.D., 2011. The regulation and physiology of mitochondrial proton leak. Physiology 26, 192–205.
Druzhyna, N.M., Wilson, G.L., LeDoux, S.P., 2008. Mitochondrial DNA repair in aging and disease. Mech. Ageing Dev. 129, 383–390.
Du, Z., Hu, Y., Yang, Y., Sun, Y., Zhang, S., Zhou, T., Zeng, L., Zhang, W., Huang, X., Kong, W., Zhang, H., 2012b. NADPH oxidase-dependent oxidative stress and mitochondrial damage in hippocampus of D-galactose-induced aging rats. J. Huazhong Univ. Sci. Technol. - Med. Sci. 32, 466–472.
Du, Z., Yang, Y., Hu, Y., Sun, Y., Zhang, S., Peng, W., Zhong, Y., Huang, X., Kong, W., 2012a. A long-term high-fat diet increases oxidative stress, mitochondrial damage and apoptosis in the inner ear of D-galactose-induced aging rats. Hear. Res. 287, 15–24.
Du, Z., Yang, Q., Liu, L., Li, S., Zhao, J., Hu, J., Liu, C., Qian, D., Gao, C., 2015. NADPH oxidase 2-dependent oxidative stress, mitochondrial damage and apoptosis in the ventral cochlear nucleus of D-galactose-induced aging rats. Neuroscience 286, 281–292.
el, B.J., Faust, L.P., Babior, B.M., 1994. The phosphorylation of the respiratory burst oxidase component p47phox during neutrophil activation. Phosphorylation of sites recognized by protein kinase C and by proline-directed kinases. J. Biol. Chem. 269, 23431–23436.
El, B.J., Faust, R.P., Johnson, J.L., Babior, B.M., 1996. Phosphorylation of the respiratory burst oxidase subunit p47phox as determined by two-dimensional phosphopeptide mapping. Phosphorylation by protein kinase C, protein kinase A, and a mitogen-activated protein kinase. J. Biol. Chem. 271, 6374–6378.
Frisina, R.D., Walton, J.P., 2006. Age-related structural and functional changes in the cochlear nucleus. Hear. Res. 216–217, 216–223.
Green, D.R., Kroemer, G., 2004. The pathophysiology of mitochondrial cell death. Science 305, 626–629.
Harman, D., 2001. Aging: overview. Ann. N. Y. Acad. Sci. 928, 1–21.
Hengartner, M.O., 2000. The biochemistry of apoptosis. Nature 407, 770–776.
Hiona, A., Leeuwenburgh, C., 2008. The role of mitochondrial DNA mutations in aging and sarcopenia: implications for the mitochondrial vicious cycle theory of aging. Exp. Gerontol. 43, 24–33.
Humes, L.E., Dubno, J.R., Gordon-Salant, S., Lister, J.J., Cacace, A.T., Cruickshanks, K.J., Gates, G.A., Wilson, R.H., Wingfield, A., 2012. Central presbycusis: a review and evaluation of the evidence. J. Am. Acad. Audiol. 23, 635–666.
Johnson, D.K., Schillinger, K.J., Kwait, D.M., Hughes, C.V., McNamara, E.J., Ishmael, F., O'Donnell, R.W., Chang, M.M., Hogg, M.G., Dordick, J.S., Santhanam, L., Ziegler, L.M., Holland, J.A., 2002. Inhibition of NADPH oxidase activation in endothelial cells by ortho-methoxy-substituted catechols. Endothelium 9, 191–203.
Kapoor, M., Sharma, N., Sandhir, R., Nehru, B., 2018. Effect of the NADPH oxidase inhibitor apocynin on ischemia-reperfusion hippocampus injury in rat brain. Biomed. Pharmacother. 97, 458–472.
Kashiwagi, A., Shinozaki, K., Nishio, Y., Maegawa, H., Maeno, Y., Kanazawa, A., Kojima, H., Haneda, M., Hidaka, H., Yasuda, H., Kikkawa, R., 1999. Endothelium-specific activation of NAD(P)H oxidase in aortas of exogenously hyperinsulinemic rats. Am. J. Physiol. 277, E976–E983.
Kleniewska, P., Piechota, A., Skibska, B., Gorąca, A., 2012. The NADPH oxidase family and its inhibitors. Arch. Immunol. Ther. Exp. 60, 277–294.
Kumar, A., Dogra, S., Prakash, A., 2009. Effect of carvedilol on behavioral, mitochondrial dysfunction, and oxidative damage against D-galactose induced senescence in mice. Naunyn-Schmiedeberg's Arch. Pharmacol. 380, 431–441.
Leto, T.L., Morand, S., Hurt, D., Ueyama, T., 2009. Targeting and regulation of reactive oxygen species generation by Nox family NADPH oxidases. Antioxidants Redox Signal. 11, 2607–2619.
Li, G., Yu, J., Zhang, L., Wang, Y., Wang, C., Chen, Q., 2018. Onjisaponin B prevents cognitive impairment in a rat model of D-galactose-induced aging. Biomed. Pharmacother. 99, 113–120.
Lu, J., Wu, D.M., Zheng, Y.L., Hu, B., Zhang, Z.F., 2010. Purple sweet potato color alleviates D-galactose-induced brain aging in old mice by promoting survival of neurons via PI3K pathway and inhibiting cytochrome C-mediated apoptosis. Brain Pathol. 20, 598–612.
Lu, X.Y., Wang, H.D., Xu, J.G., Ding, K., Li, T., 2014. NADPH oxidase inhibition improves neurological outcome in experimental traumatic brain injury. Neurochem. Int. 69, 14–19.
Mailloux, R.J., Harper, M.E., 2011. Uncoupling proteins and the control of mitochondrial reactive oxygen species production. Free Radic. Biol. Med. 51, 1106–1115.
Markaryan, A., Nelson, E.G., Hinojosa, R., 2009. Quantification of the mitochondrial DNA common deletion in presbycusis. Laryngoscope 119, 1184–1189.
Meissner, C., Bruse, P., Mohamed, S.A., Schulz, A., Warnk, H., Storm, T., Oehmichen, M., 2008. The 4977 bp deletion of mitochondrial DNA in human skeletal muscle, heart and different areas of the brain: a useful biomarker or more. Exp. Gerontol. 43, 645–652.
Mohammed, A.M., Kowluru, A., 2013. Activation of apocynin-sensitive NADPH oxidase (Nox2) activity in INS-1 832/13 cells under glucotoxic conditions. Islets 5, 129–131.
Nicklas, J.A., Brooks, E.M., Hunter, T.C., Single, R., Branda, R.F., 2004. Development of a quantitative PCR (TaqMan) assay for relative mitochondrial DNA copy number and the common mitochondrial DNA deletion in the rat. Environ. Mol. Mutagen. 44, 313–320.
Okamura, N., Curnutte, J.T., Roberts, R.L., Babior, B.M., 1988. Relationship of protein phosphorylation to the activation of the respiratory burst in human neutrophils. Defects in the phosphorylation of a group of closely related 48-kDa proteins in two forms of chronic granulomatous disease. J. Biol. Chem. 263, 6777–6782.
Olukman, M., Orhan, C.E., Celenk, F.G., Ulker, S., 2010. Apocynin restores endothelial dysfunction in streptozotocin diabetic rats through regulation of nitric oxide synthase and NADPH oxidase expressions. J. Diabetes Complicat. 24, 415–423.
Prabhulkar, S., Li, C.Z., 2010. Assessment of oxidative DNA damage and repair at single cellular level via real-time monitoring of 8-OHdG biomarker. Biosens. Bioelectron. 26, 1743–1749.
Rehman, S.U., Shah, S.A., Ali, T., Chung, J.I., Kim, M.O., 2017. Anthocyanins reversed D-galactose-induced oxidative stress and neuroinflammation mediated cognitive impairment in adult rats. Mol. Neurobiol. 54, 255–271.
Roth, T.N., 2015. Aging of the auditory system. Handb. Clin. Neurol. 129, 357–373.
Rotrosen, D., Leto, T.L., 1990. Phosphorylation of neutrophil 47-kDa cytosolic oxidase factor. Translocation to membrane is associated with distinct phosphorylation events. J. Biol. Chem. 265, 19910–19915.
Song, S.X., Gao, J.L., Wang, K.J., Li, R., Tian, Y.X., Wei, J.Q., Cui, J.Z., 2013. Attenuation of brain edema and spatial learning deficits by the inhibition of NADPH oxidase activity using apocynin following diffuse traumatic brain injury in rats. Mol. Med. Rep. 7, 327–331.
Stefanska, J., Pawliczak, R., 2008. Apocynin: Molecular Aptitudes. Mediators Inflamm. vol. 2008. pp. 106507.
Sun, H.Y., Hu, Y.J., Zhao, X.Y., Zhong, Y., Zeng, L.L., Chen, X.B., Yuan, J., Wu, J., Sun, Y., Kong, W., Kong, W.J., 2015. Age-related changes in mitochondrial antioxidant enzyme Trx2 and TXNIP-Trx2-ASK1 signal pathways in the auditory cortex of a mimetic aging rat model: changes to Trx2 in the auditory cortex. FEBS J. 282, 2758–2774.
Toda, C., Diano, S., 2014. Mitochondrial UCP2 in the central regulation of metabolism. Best Pract. Res. Clin. Endocrinol. Metabol. 28, 757–764.
Ueda, N., Oshima, T., Ikeda, K., Abe, K., Aoki, M., Takasaka, T., 1998. Mitochondrial DNA deletion is a predisposing cause for sensorineural hearing loss. Laryngoscope 108, 580–584.
Yowe, D.L., Ames, B.N., 1998. Quantitation of age-related mitochondrial DNA deletions in rat tissues shows that their pattern of accumulation differs from that of humans. Gene 209, 23–30.